Dynamic Impact Behavior of 6061-T6 and 5083-H131 Aluminum alloys

A.G Odeshi[1], M.N. Bassim[2], M. Bolduc[3]
[1] *Department of Mechanical Engineering, University of Saskatchewan, Saskatoon, Canada,* [2]*Department of Mechanical and Manufacturing Engineering, University of Manitoba, Winnipeg, Canada;* [3]*Defense Research and Development Canada, Valcartier, Quebec, Canada;*

ABSTRACT
The results of a comparative study on microstructural evolution and damage in 6061-T6 and 5083-H131 aluminum alloys tested at high strain rates are discussed. Cylindrical samples of these alloys were tested in compression using instrumented direct impact Hopkinson Bar. Retention of heat and intense thermal softening along narrow bands during impact resulted in inhomogeneous deformation caused by shear strain localization along these bands. Deformed bands consisting of highly distorted and elongated grains were observed in the Aluminum 5083-H131 alloy after high velocity impact. On the other hand, adiabatic shear bands that look similar to the white etching bands commonly found in hardened steels were observed in the Aluminum 6061-T6 alloy. Whereas grain coarsening occurred inside the adiabatic shear bands in the Aluminum 5083-H131 alloy, the adiabatic shear bands in Aluminum 6061-T6 alloy were observed to contain much finer grains than the bulk material.

1. INTRODUCTION
Shear strain localization leading to formation of adiabatic shear bands is the dominant deformation mechanism at high strain rates. Adiabatic shear banding is not only commonly reported in metallic materials at high strain rates [1-3], several investigations have also shown occurrence of adiabatic shear bands in polymers [4-6], ceramics [7-9] and composite materials [10-12]. As in all metals and alloys, occurrence of adiabatic shear bands dominates deformation and failure mechanism of aluminum alloys at high strain rates. Failure of Aluminum 7075 alloy under external explosive loading is initiated by formation of adiabatic shear bands which is strongly influenced by the stress state [13]. Investigations on occurrence of adiabatic shear bands in equal channel angular pressed Aluminum 7075 alloy shows that the size of secondary precipitates plays an important role on the formation of adiabatic shear bands in this alloy under dynamic torsional loading [14]. It has also been reported that the fine secondary precipitates in the aluminum alloy matrix play a prominent role in initiation of adiabatic shear bands in alumina particle reinforced Aluminum 6061-T6 composites in torsion [15]. A comparative study of dynamic response of Aluminum 7039 and 2090 to ballistic impact showed that adiabatic shear bands are more easily formed in Aluminum 7039 alloy [16,17]. A critical strain-rate and a critical strain are reported in aluminum-lithium alloys for the occurrence of adiabatic shear bands [18]. Nanocrystallites, promoted by recrystallization effect of adiabatic heating, are observed inside adiabatic shear bands in an $Al_{90}Fe_5Gd_5$ alloy that is subjected to

high strain rate loading, both in torsion and in compression [19]. In the present study, the dynamic response of Aluminum 6061-T6 and 5083-H131 alloys to impact loading is investigated. The mechanism of failure as it relates to shear strain localization and occurrence of adiabatic shear band is discussed.

2. MATERIALS AND METHODS

The materials investigated in this study are Aluminum 6061-T6 and 5083-H131 alloys. Cylindrical specimens of these materials, 9.5 mm in diameter and 10.5 mm long, were subjected to dynamic mechanical loading in compression at high strain rates using a direct impact Hopkinson bar system (Fig. 1). The specimens were attached to the transmitter bar using wax. The wax serves the purpose of attaching the specimen to the output bar and at the same time acting as lubricant, which reduces the friction between the bar and the specimen. This leads to reduction in buckling effect during deformation. The cylindrical rod specimen was impacted by a projectile made of a quench hardened high strength alloy steel weighing 1.905 kg and having a hardness value of 47 HRC. The striker bar has a length and diameter of 38 and 225 mm respectively. The impact velocity was about 19 m/s. The elastic waves generated in the test piece during impact propagate through the material, and are captured by the stain gages attached to the output bar, which is made of AISI 4340 steel, also with a diameter of 38 mm. These elastic waves data are conditioned and amplified by a signal conditioner/amplifier connected to the strain gage. A 200 MHz mixed signal oscilloscope connected to the signal conditioner/amplifier recorded and stored the elastic wave data. These are used in generating the dynamic stress-strain curves. Assuming constant volume and a linear variation of displacement with time and constant strain rate, the true stress (σ) and true strain (ε) at time t are given by the following expressions:

$$\varepsilon_{(t)} = \ln \frac{L_i}{L_i - (L_i - L_f)(t/t_f)} \tag{1}$$

$$\sigma_{(t)} = \frac{P_{(t)}}{A_i} \frac{L_i - (L_i - L_f)(t/t_f)}{L_i} \tag{2}$$

where L_i and L_f are initial and final lengths respectively, t_f is the deformation time, $P_{(t)}$ is the applied load at time t and A_i is the original cross-section area of the test specimen.

After impact, the specimens were subjected to microscopic investigations to determine the microstructural evolution in the two alloys under the impact loading. The etching reagent used for both alloys consist of 25ml Methanol, 25 ml HCl, 25 ml HNO_3 and 1 drop HF.

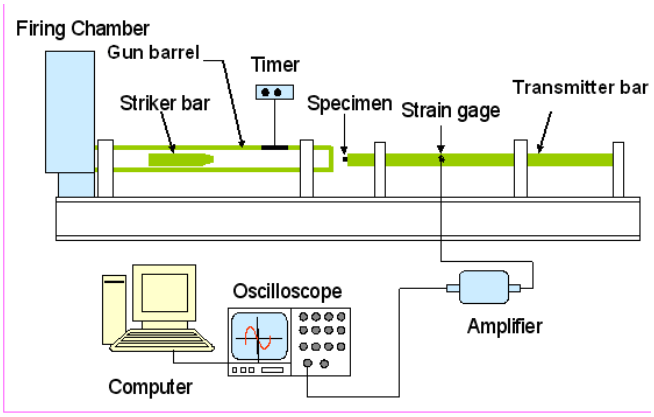

Fig. 1: A sketch of the direct impact Hopkinson bar used in this investigation

2. RESULTS AND DISCUSSION

Typical dynamic stress strain curves obtained from the dynamic impact tests are shown in Fig. 2. Under the dynamic impact loading, the Aluminum 5083-H131 alloy shows a slightly higher strength and a lower total strain compared to Aluminum 6061-T6 alloy. The initial strain hardening effect of plastic deformation before the onset of thermal softening effect of adiabatic heating is higher in the Aluminum 5083-H131 alloy than in the Aluminum 6061-T6 alloy. The difference in the initial strain hardening effect becomes first noticeable at stress and strain levels above 400 MPa and 0.05, respectively. The dynamic stress-strain curves for both alloys are collinear until thermal softening beginning to play a more dominant role in the deformation of the Aluminum 6061-T6 alloy. At strain value in excess of 0.3, adiabatic heating leading to intense shear strain localization and adiabatic shear banding begins to dominate the deformation process in both alloys. The dynamic stress strain curves of the two investigated aluminum alloys show that the effect of adiabatic heating is more pronounced in the Aluminum 6061-T6 alloy than in the Aluminum 5083-H131 alloy.

Microscopic investigations of the impacted specimens show that shear strain localization leading to occurrence of adiabatic shear bands play a significant role at the later stage of deformation. The two typical adiabatic shear bands observed on the transverse section of an impacted cylindrical sample of the Aluminum 5083-H131 alloy are shown in Fig 3. One has a circular shape while the other is linear. The circular-shaped bands (Fig. 3a) propagate along a circular path at a radial distance of 0.8 - 1.2 mm from the circumferential surface of the cylindrical test specimens. The linear bands (Fig. 3b) propagate linearly across the transverse section of the test specimens. The circular shear bands which are concentric to the circumference of the test specimens are much wider than the linear bands. In some cases, bifurcation of the linear adiabatic shear bands was observed as documented in Fig. 3c. Deformed shear bands that typically occur in non-ferrous alloys were observed in the Aluminum 5083-H131 alloy. The deformed bands consist of elongated and distorted grains caused by high strain intensity inside the shear bands.

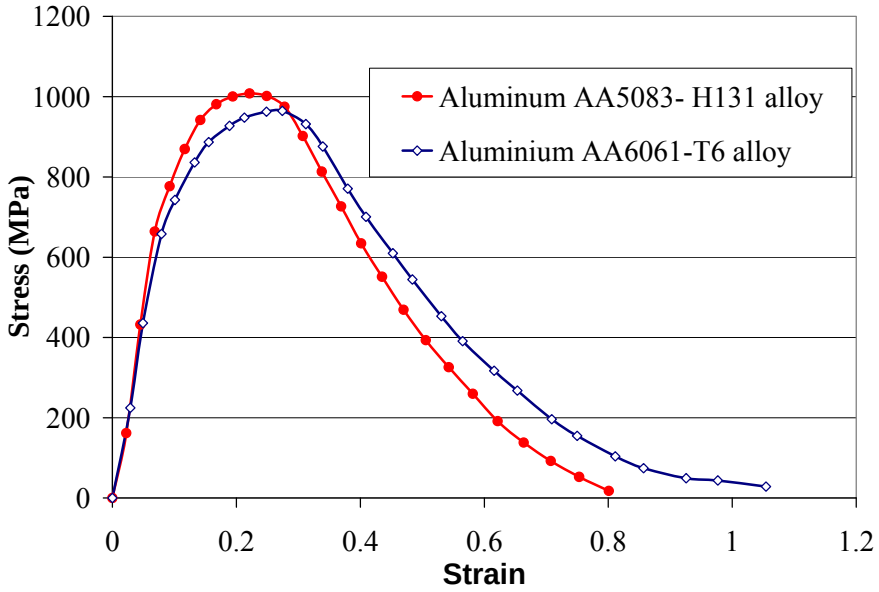

Fig. 2: Typical stress strain curves for the investigated alloys under dynamic impact loading.

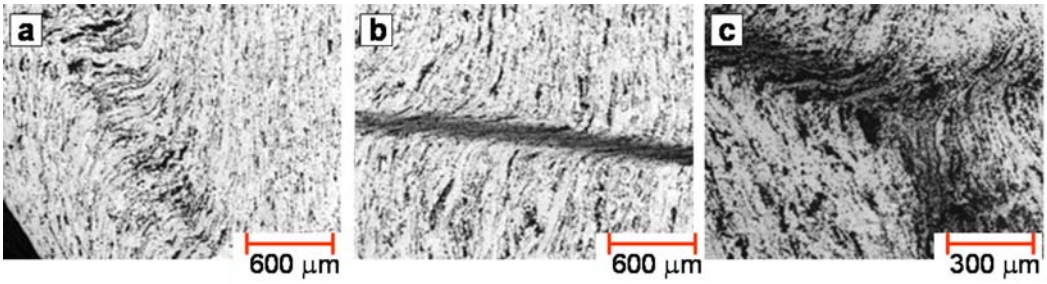

Fig. 3: Adiabatic shear bands on transverse section of an impacted cylinder of 5083-H131 aluminum alloy: (a) circular band, (b) linear band and (c) bifurcation of a linear shear band.

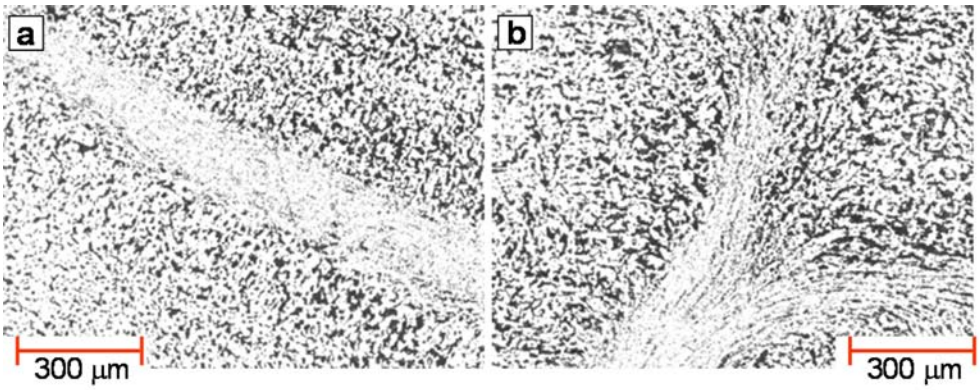

Fig. 4: Adiabatic shear bands on a transverse section of an impacted cylindrical specimen of 6061-T6 aluminum alloy (a) white ASB similar to the one commonly observed in steels (c) bifurcation of a shear band.

The morphology of the adiabatic shear bands observed in the Aluminum 6061-T6 under the same impact condition is different from those observed in Aluminum 5083-H131 alloy. Adiabatic shear bands observed in the Aluminum 6061-T6 alloy are characteristically white (Fig. 4). They are similar to the white etching bands (also called transformed bands) which are commonly observed in steels and titanium alloys. Xu *et al*. [20] have also reported the occurrence of white etching adiabatic shear bands in an aluminum-lithium alloy. This type of shear bands is however not commonly reported in most aluminum alloys. The white adiabatic shear bands observed in the Aluminum 6060-T6 alloy in this study cannot be regarded as transformed bands, because solid phase transformation typical of martensitic transformation is not expected in this alloy. The observation of white adiabatic shear bands in aluminum alloy thus raise pertinent questions on the suggestion that the white shear bands in steel is attributable to austenitization followed by martensitic transformation inside the shear bands at high strain rates. As in Aluminum 5083-H131 alloy, bifurcation of the white shear bands was also observed in Aluminum 6061-T6 alloy (Fig. 4b). The shear bands were observed to terminate shortly after bifurcation. The white shear bands in Aluminum 6061-T6 are parabolic in shape and no linear band was observed on transverse sections of this alloy as reported for Aluminum 5083-H131.

Adiabatic shear bands form as a result of adiabatic heating whereby the heat generated along the shear band region is not conducted away. This leads to considerable temperature increase, intense thermal softening and strength loss along the path of heat wave. Aluminum 5083-H131 is a strain-hardened alloy. Therefore, dynamic recovery of the internal strain could also contribute to the strength loss in the shear band region. The consequence of the strength loss is the intensely localised shear deformation that brings about the observed grain distortion in the deformed bands in the impacted Aluminum 5083-H131 alloy. Figure 5 shows optical micrographs that indicate coarse grains inside the shear bands region compared to the region outside the shear band in the Aluminum 5083-H131 alloy. This suggests a remarkable grain growth as a result temperature rise in the shear bands during impact.

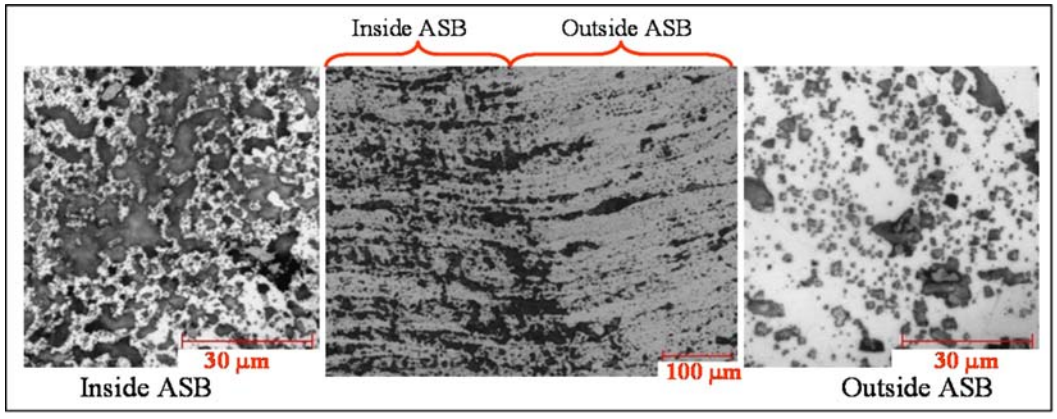

Fig. 5: Optical micrographs showing microstructure inside and outside adiabatic shear band (ASB) in Aluminum 5083-H131 alloy

Whereas grains-coarsening occurred inside the adiabatic shear bands in the Aluminum 5083-H131 alloy, finer grains were observed inside the shear bands in Aluminum 6061-T6 alloy in comparison to the regions outside the shear band (Fig. 6). It is suggested that the high intensity of shear strain induced grain fragmentation inside the shear band in the Aluminum 6061-T6 alloy during impact. Grain fragmentation has also been reported as one of the mechanisms used to explain microstructural evolution leading to occurrence of white etching bands in steels [21]. Dislocation generation, redistribution and patterning leading to formation of dislocation cells of a few hundreds nanometre sizes have also been suggested as the mechanism for the formation of ultra-fine equiaxed cells in white adiabatic shear bands in α-titanium [22]. Meyers *et al.* [23] reported that the microstructural evolution at high strain rates begin with a homogeneous distribution of dislocations that rearrange themselves into dislocation cells which eventually become elongated sub-grains and subsequently break down into equi-axed microcrystalline structure as strain increases.

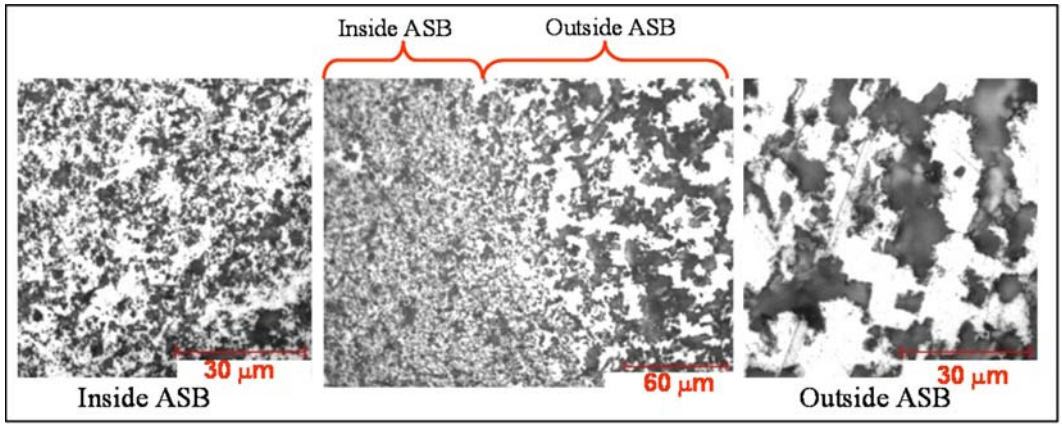

Fig. 6: Optical micrographs showing microstructure inside and outside adiabatic shear band (ASB) in Aluminum 6061-T6 alloy

Armstrong *et al.* [1,24] proposed a dislocation pile-up avalanche model to explain the occurrence of extremely fine sub-grains in transformed bands and used the model to explain the difference in the susceptibility of fcc and bcc metals to adiabatic shear banding. Xu *et al.* [20] suggested dynamic recrystallisation as the mechanism of formation of fine equi-axed grains observed in white etching bands in a peak age-hardened 8090 Aluminum-Lithium alloys. Aluminum 6061-T6 is a precipitation-hardened alloy and the presence of secondary precipitates in this alloy could increase its susceptibility to adiabatic shear banding, especially its susceptibility to the formation of white shear bands. It has been suggested that the presence of hard secondary precipitates or inhomogeneities in microstructure plays a significant role in the initiation of adiabatic shear bands in metallic alloys [2, 14]. This explains why adiabatic shear bands are more fully developed in this alloy than in the strain-hardened Aluminum 5083-H131 alloy.

3. CONCLUSION

The response of Aluminum 6061-T6 and 5083-H131 alloys to dynamic mechanical loading at high strain rates is investigated. Adiabatic heating and shear strain localization dominates the plastic deformation of both alloys at high strain rates. The results of these investigations show that Aluminum 6061-T6 is more susceptible to adiabatic shear band formation than Aluminum 5083-H131 alloy. Whereas deformed bands were formed in the Aluminum 5083-H131 alloy, white shear bands similar to the transformed bands that commonly occur in ferrous and titanium alloys were observed in the Aluminum 6061-T6 alloy. Grain coarsening occurred in the deformed bands in Aluminum 5083-H131 alloy while grain refinement was observed inside the adiabatic shear bands in Aluminum 6061-T6 alloy.

ACKNOWLEDGEMENTS

The authors wish to thank the Natural Science and Engineering Research Council of Canada (NSERC) and Defense Research and Development Canada (DRDC) for their financial support of this study.

REFERENCES

[1] R.W Armstrong, S.M. Walley, High strain-rate properties of metals and alloys, International Materials Reviews 53 (2008) 105-128.

[2] M.N. Bassim, Study of the formation of adiabatic shear bands in steels, Journal of Materials Processing Technology 119 (2001) 234-236.

[3] Q. Xue, G.T. Gray, Development of adiabatic shear bands in annealed 316L stainless steel. Part I. Correlation between evolving microstructure and mechanical behavior, Metallurgical and Materials Transactions A 37 (2006) 2435-46.

[4] T. Bjerke and J. Lambros, Heating during shearing and opening dominated dynamic fracture of polymers, Experimental Mechanics 42 (2002) 107-114.

[5] K. Ravi-Chandar, J. Lu, B. Yang and Z. Zhu, Failure mode transitions in polymers under high strain rate loading, International Journal of Fracture 101 (2000) 33-72.

[6] Z. Bin Ahmad and M. F. Ashby, Failure-mechanism maps for engineering polymers, Journal of Materials Science 23 (1988) 2037-2050.

[7] V.F. Nesterenko, M.A. Meyers and H.C Chen, Shear localization in high-strain-rate deformation of granular alumina, Acta Materialia 44 (1996). 2017-26.

[8] C.J. Shih, M.A Meyers, V.F. Nesterenko, High-strain-rate deformation of granular silicon carbide, Acta Materialia 46 (1998) 4037-4065.

[9] C.J. Shih, V.F. Nesterenko and M.A. Meyers, High-strain-rate deformation and comminution of silicon carbide, Journal of Applied Physics 83 (1998). 4660-4671.

[10] L. H. Dai , L. F. Liu and Y. L. Bai, Effect of particle size on the formation of adiabatic shear band in particle reinforced metal matrix composites, Materials Letters 58 (2004) 1773 -1776.

[11] G.M Owolabi, A.G. Odeshi, M.N.K Singh and M.N.Bassim, Dynamic shear band formation in Aluminum 6061-T6 and Aluminum 6061-T6/Al_2O_3 composites, Materials Science and Engineering A 457 (2007) 114-119.
[12] A. J. Wagoner Johnson, K. S. Kumar and C. L. Briant, Deformation mechanisms in Ti-6Al-4V/TiC composites, Metallurgical and Materials Transactions A 34 (2003) 1869-1877.
[13] Y. Yang, Y. Zeng, D.H. Li and M. Li, Damage and fracture mechanism of aluminum alloy thick-walled cylinder under external explosive loading, Materials Science and Engineering A, 490 (2008) 378-384.
[14] Y. G. Kim, B. Hwang, S. Lee, W. G. Kim, D. H. Shin, Dynamic deformation and fracture behavior of ultrafine-grained aluminum alloy fabricated by equal-channel angular pressing, Metallurgical and Materials Transactions A 36 (2005) 2947-2955.
[15] C. G. Lee, Y-J Lee, S. Lee, Observation of adiabatic shear bands formed by ballistic impact in aluminum-lithium alloys, Scripta Metallurgica et Materialia 32 (1995) 821-826.
[16] A.G. Odeshi, G.M. Owolabi, M.N.K. Singh and M.N. Bassim, Deformation and fracture behavior of metal matrix composites during dynamic mechanical loading, Metallurgical and Materials Transaction A 38 (2007) 2674-2680.
[17] C.G. Lee, S. Lee, Correlation of dynamic torsional properties with adiabatic shear banding behavior in ballistically impacted aluminum-lithium alloys, Metallurgical and Materials Transactions A 29 (1998) 227-235.
[18] Y. Xu, J. Zhang, Y. Bai, M.A. Meyers, Shear localization in dynamic deformation: Microstructural evolution, Metallurgical and Materials Transactions A 39 (2008) 811-843.
[19] W.H. Jiang, M. Atzmon, The effect of compression and tension on shear-band structure and nanocrystallization in amorphous $Al_{90}Fe_5Gd_5$: A high-resolution transmission electron microscopy study, Acta Materialia 51 (2003) 4095-4105.
[20] Y.B. Xu, W. L. Zhong, Y. J. Chen, L. T. Shen, Q. Liu, Y. L. Bai and M. A. Meyers, Shear localization and recrystallization in dynamic deformation of 8090 Al–Li alloy, Materials Science and Engineering A 299 (2001) 287-295.
[21] B.K. Kad, J.-M. Gebert, M.T. Perz-Parado and M.A. Meyers, Ultra-fined grained zirconium by dynamic deformation, Acta Materialia 54 (2006) 4111-4127.
[22] D.R. Chichili, K.T. Ramesh, K.J. Hemker, Adiabatic shear localization in α-titanium alloy: experiments, modeling and structure, Journal of Mechanics and Physics of Solids 52 (2004) 1889-1909.
[23] M.A. Meyers, V.F Nesterenko, J.C. LaSalvia, M.P. Bondar, Y.J. Chen, Y.L. Lukyanov, Shear localization and recrystallization in high-strain, high-strain-rate deformation of tantalum, Material Science Engineering A 229 (1997) 23-41.

[24] R.W. Armstrong and W.R. Grisse, Hot spots from dislocation pile-up avalanches in shock compression of condensed matter (ed. Furnish et al.), America institute of Physics, Melville, NY (2006) 1033-1036.